Biochimica et Biophysica Acta 1837 (2014) 1540–1547

Contents lists available at ScienceDirect

Biochimica et Biophysica Acta

journal homepage: www.elsevier.com/locate/bbabio

The time course of non-photochemical quenching in phycobilisomes of *Synechocystis* sp. PCC6803 as revealed by picosecond time-resolved fluorimetry ☆

E.G. Maksimov [a,*], F.-J. Schmitt [b], E.A. Shirshin [c], M.D. Svirin [a], I.V. Elanskaya [d], T. Friedrich [b], V.V. Fadeev [c], V.Z. Paschenko [a], A.B. Rubin [a]

[a] Department of Biophysics, Faculty of Biology, M.V. Lomonosov Moscow State University, 119992 Moscow, Russia
[b] Institute of Chemistry, Biophysical Chemistry, TU Berlin, Straße des 17. Juni 135, D-10623 Berlin, Germany
[c] Department of Quantum Electronics, Faculty of Physics, M.V. Lomonosov Moscow State University, 119992 Moscow, Russia
[d] Department of Genetics, Faculty of Biology, M.V. Lomonosov Moscow State University, 119992 Moscow, Russia

ARTICLE INFO

Article history:
Received 31 October 2013
Received in revised form 25 December 2013
Accepted 15 January 2014
Available online 23 January 2014

Keywords:
Phycobilisome
Energy migration
Non-photochemical quenching
Fluorescence lifetime
Temperature

ABSTRACT

As high-intensity solar radiation can lead to extensive damage of the photosynthetic apparatus, cyanobacteria have developed various protection mechanisms to reduce the effective excitation energy transfer (EET) from the antenna complexes to the reaction center. One of them is non-photochemical quenching (NPQ) of the phycobilisome (PB) fluorescence. In *Synechocystis* sp. PCC6803 this role is carried by the orange carotenoid protein (OCP), which reacts to high-intensity light by a series of conformational changes, enabling the binding of OCP to the PBs reducing the flow of energy into the photosystems. In this paper the mechanisms of energy migration in two mutant PB complexes of *Synechocystis* sp. were investigated and compared. The mutant CK is lacking phycocyanin in the PBs while the mutant ΔPSI/PSII does not contain both photosystems. Fluorescence decay spectra with picosecond time resolution were registered using a single photon counting technique. The studies were performed in a wide range of temperatures — from 4 to 300 K. The time course of NPQ and fluorescence recovery in darkness was studied at room temperature using both steady-state and time-resolved fluorescence measurements. The OCP induced NPQ has been shown to be due to EET from PB cores to the red form of OCP under photon flux densities up to 1000 μmol photons m^{-2} s^{-1}. The gradual changes of the energy transfer rate from allophycocyanin to OCP were observed during the irradiation of the sample with blue light and consequent adaptation to darkness. This fact was interpreted as the revelation of intermolecular interaction between OCP and PB binding site. At low temperatures a significantly enhanced EET from allophycocyanin to terminal emitters has been shown, due to the decreased back transfer from terminal emitter to APC. The activation of OCP not only leads to fluorescence quenching, but also affects the rate constants of energy transfer as shown by model based analysis of the decay associated spectra. The results indicate that the ability of OCP to quench the fluorescence is strongly temperature dependent. This article is part of a Special Issue entitled: Photosynthesis Research for Sustainability: Keys to Produce Clean Energy.

1. Introduction

Cyanobacteria are autotrophic organisms that efficiently use the energy of solar radiation by various light absorbing pigments. The photosynthetic apparatus of cyanobacteria consists of several pigment–protein complexes, which have optimized during billion years of evolution [1,2]. Like higher plants, cyanobacteria comprehend the photosystems I and II, and, in addition, they developed special supramolecular complexes — phycobilisomes (PBs), which allow them to increase the efficiency of light collection [3]. PBs consist of various phycobiliproteins — pigment–protein complexes of similar structure containing a different

Abbreviations: PBs, phycobilisomes; CK_PBs, phycobilisome cores from CK mutant; PCB, phycocyanobilin; PC, phycocyanin; APC, allophycocyanin; TE, terminal emitter; PS II, photosystem II; ROS, reactive oxygen species; NPQ, non-photochemical quenching; OCP, orange carotenoid protein; FRP, fluorescence recovery protein; τ, fluorescence lifetime; φ_{fl}, fluorescence quantum yield; TCSPC, time-correlated single photon counting; DAS, decay associated spectra; FWHM, full width at half maximum; PDB, protein data bank

☆ This article is part of a Special Issue entitled: Photosynthesis Research for Sustainability: Keys to Produce Clean Energy.

* Corresponding author.
E-mail address: emaksimoff@yandex.ru (E.G. Maksimov).

0005-2728/$ – see front matter © 2014 Published by Elsevier B.V.
http://dx.doi.org/10.1016/j.bbabio.2014.01.010

number of chromophores, depending on the class of the certain phycobiliprotein. All phycobiliproteins contain α- and β-polypeptide subunits, which covalently bind phycobilin chromophores, represented by linear tetrapyrroles. The PBs of *Synechocystis* show a typical hemispheroid structure composed by phycocyanin (PC), allophycocyanin (APC_{660}), and a set of different terminal emitters (TE or APC_{680}). APC and TE form the so-called core of the PBs which is connected to the stromal surface of the thylakoid membrane, located in the center of a semidisk, and presented by three cylinders (see Fig. 1). In addition, six cylinders formed by hexameric disks of PC are attached to the core. Such structures enable cyanobacteria to absorb light over a wide spectral range with high efficiency and transfer the excitation energy to chlorophyll (see Fig. 2), thus increasing the effective absorption cross section of the photosystems in the spectral region where chlorophyll absorption is not effective [4,5].

However, high levels of solar radiation may cause damage of photosynthetic membranes and pigment–protein complexes mostly due to the increasing probability of the formation of reactive oxygen species (ROS) [6]. Since the reparation of damaged membranes and proteins requires significant energy and resources, cyanobacteria have developed a special protection mechanism — the non-photochemical quenching (NPQ) of the PB excitation [7]. Recent studies have shown that the sensor, regulator and effector of NPQ in cyanobacteria are a 35 kDa water-soluble orange carotenoid protein (OCP) [8–10]. Activation of NPQ is a multi-step process [11,12]. OCP contains special carotenoid (3′-hydroxyechinenone), which is capable of changing its conformation as a result of the absorption of photons in the 400–550 nm spectral range, resulting in the transition of OCP from its orange (OCP^O) to the red form (OCP^R) [7,13]. It was shown that only OCP^R interacts with PBs and reduces the intensity of phycobiliprotein fluorescence, thus diminishing the flow of energy through the photosystems [14]. It was also concluded that the quenching is most likely caused by charge transfer between APC_{660} of the core and the OCP carotenoid in its activated red form, and the energy transfer rate from the excited APC_{660} to OCP^R is ultrafast ($\sim 240 \pm 60\ fs^{-1}$) [15,16]. A specific partner protein – fluorescence recovery protein (FRP) – is involved into conversion of OCP^R back to OCP^O in cyanobacterial cells [17].

The mechanism of interaction between OCP and PBs is still under discussion. The fact that *in vivo* the ratio of OCP to PBs is usually less than unity raises questions about the existence of a specific site of PBs responsible for interaction with OCP [16,18,19]. Another fact, that there are only few specific molecules like terminal emitters, including the linker polypeptide, presented in the core of PBs (compared to tens or hundreds of molecules of APC and PC), raises the possibility of a selective interaction of OCP molecule with the specific site of the PB core [13,20,21]. However, a clear answer to these questions does not exist yet in the scientific literature, due to the complexity of the photosynthetic apparatus and NPQ process.

There is a trend in literature to study the NPQ process by dividing the complex *in vivo* cell systems into separate fragments. Our previous publication was devoted to the study of conformational mobility of individual phycobiliproteins in different environments [22]. It was shown that the spectral characteristics of the phycobiliprotein fluorescence have complex temperature dependence and are sensitive to the rate of freezing. These results allowed us to perform accurate low temperature experiments for the study of energy migration in PBs and NPQ in cyanobacteria in this work. To perform these tasks, the cyanobacterium *Synechocystis* sp. PCC6803 was chosen, allowing the creation of different mutants, characterized by a well-defined set of properties [23–25] due to the fully sequenced genome. The gene engineering approach combined with techniques of protein purification allows one to significantly reduce the number of EET stages presented in Fig. 2 and to perform a separate analysis of certain EET stages which is necessary to get unambiguous results from modeling the EET [26]. In this work we present a study of the energy migration in the PB core, and the dynamics of OCP triggered NPQ in ΔPSI/PSII mutant lacking both photosystems. All experimental results are accompanied by the model based evaluation due to the EET scheme as shown in Fig. 2.

2. Materials

The cells of the cyanobacterium *Synechocystis* sp. PCC 6803 were grown in modified BG-11 medium [27] at 30 °C under luminescent

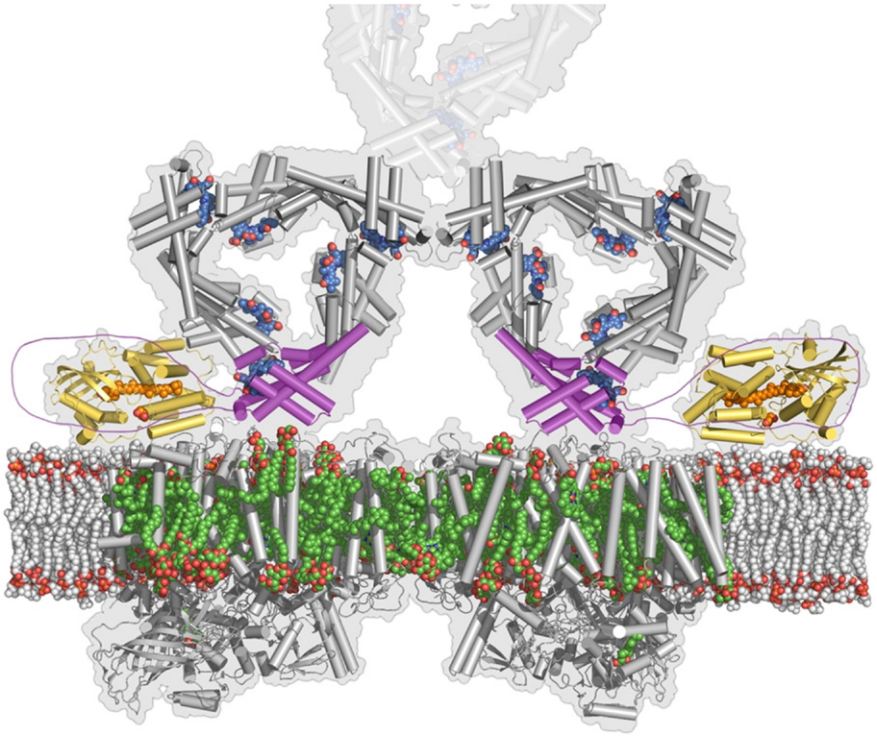

Fig. 1. Schematic representation of photosynthetic membranes of the CK mutant (lacking PC) of *Synechocystis* sp. PCC6803. The chlorophylls of PS II are shown in green, the OCP is shown in yellow and orange, The Lcm linker-polypeptide is shown in purple. The structures of OCP, APC and PS II are taken from the PDB (1M98, 1ALL and 3KZI, respectively).

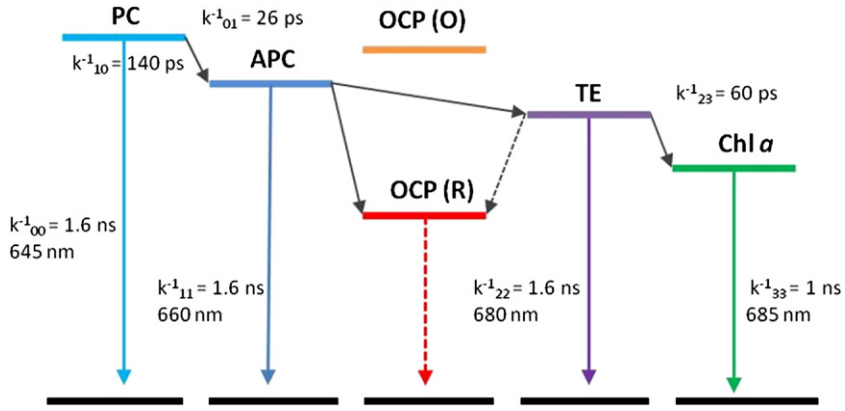

Fig. 2. Energy migration in phycobilisomes of *Synechocystis* sp. PCC6803. Detailed explanation in review [39].

lamps with white light illumination at constant light exposure of 40 μmol photons m^{-2} s^{-1}. CK mutant (Δ*cpcBAC1C2*), lacking PC [23] was grown in BG-11 culture medium at doubled concentration of $NaNO_3$ in the presence of 80 μg/ml kanamycin. ΔPSI/ΔPSII mutant (Δ*psaAB*/Δ*psbDIC*/Δ*psbDII*), lacking PSI and PSII, was cultivated in BG-11 medium, containing glucose (10 mM), spectinomycin (25 μg/ml), erythromycin (20 μg/ml) and chloramphenicol (20 μg/ml) at light exposure of 5 μmol photons m^{-2} s^{-1} [28,29].

PB cores were isolated from the CK mutant (CK_PBs) according to the procedure described in [20].

3. Methods

Fluorescence measurements were performed using time- and wavelength-correlated single photon counting using the equipment described in [26,30]. The setup included a registration system with a 16-channel multi-anode photomultiplier tube (Hamamatsu R5900) with 16 separate anode elements and a common cathode and dynode system integrated in form of a "grating mesh" (PML-16C, Becker&Hickl, Berlin, Germany). The polychromator was equipped with a 600 or 1200 grooves/mm grating resulting in a spectral bandwidth of the PML-16C of about 200 or 100 nm (resolution of 12.5 to 6.25 nm/channel, respectively). Excitation was performed with a pulsed 405 nm laser diode (IOS, Saint Petersburg, Russia) delivering 13 pJ, 26 ps FWHM pulses, driven at a repetition rate of 50 MHz. For steady-state fluorescence measurements we used FluoroMax-4 (Horiba Jobin Yvon, France) and a USB-connected system with CCD array USB4000 (Ocean Optics, USA). Absorption spectra were recorded using a USB2000 spectrometer with DT-MINI-2-GS deuterium tungsten halogen light source (Ocean Optics, USA).

The ΔPSI/PSII mutant samples were rapidly frozen in liquid nitrogen as described below. A reservoir connected to the sample via heat conducting material was filled with liquid nitrogen. The temperature was decreased at a rate of 2–3 °C per second so that the minimum value of 77 K was reached within several minutes. The subsequent temperature increase started after evaporation of liquid nitrogen, due to heat exchange with the environment, reaching room temperature (25 °C) within ~120 min. Simultaneously with the temperature increase, the fluorescence decay curves were recorded at intervals of 10–15 °C. Since the temperature increased by 0.5–2 °C during the time of the measurement, each point on the plots corresponds to the averaged temperature interval. The described method of fast freezing allows investigations of the temperature dependency of the fluorescence properties of samples in the range between 77 K and 300 K [22].

The experiments with CK_PBs were performed in the temperature range between 10 K and room temperature by using a custom-built variable-temperature closed loop helium cryostat (10–300 K, CTI-Cryogenics 8001/8300, Germany) as described in [26]. To prevent the PB damage due to slow freezing [22,31] the samples of CK_PBs were incubated in 50% glycerol.

The dynamics of blue light-induced fluorescence quenching in the ΔPSI/ΔPSII mutant and the subsequent fluorescence recovery dynamics were studied using the single photon counting setup with a flow cell. To induce NPQ, the50 ml reservoir with the sample was irradiated with blue light LEDs (emission maximum at 475 nm) providing photon flux densities from 200 to7000 μmol photons m^{-2} s^{-1}. Simultaneously, the sample was pumped through the flow cell, where the sample was excited by laser pulses (405 nm, 50 MHz, 26 ps, 13 pJ) with low intensity (~2 μmol photons m^{-2} s^{-1}). The fluorescence signal was recorded during 64 cycles (f(t, T) mode of B&H SPC [30]). This setup allowed us to record the fluorescence dynamics during the transition of the samples from the dark adapted to the light adapted state and vice versa, by measuring the fluorescence intensities and lifetimes in both described configurations. Each experiment provided 1024 fluorescence decay curves (16 wavelength sections and 64 time slices).

The fluorescence decay curves were approximated by a sum of exponential decay functions. To compare between different patterns of the NPQ time course, we calculated the average decay time according to the expression:

$$\tau_{av} = \sum_i^n \tau_i a_i, \quad (1)$$

where τ_i and α_i are the lifetime and the amplitude (normalized to unity: $\sum_i^n a_i = 1$) of the i-th fluorescence decay component. To obtain the time integrated fluorescence spectra, the number of photons in each spectral channel was summed up.

The efficiency and rate of excitation energy transfer (EET) was obtained from the analysis of decay-associated spectra (DAS) calculated from the fluorescence decay curves in the spectral range between 600 and 700 nm according to the following procedure. The transient fluorescence emission traces in different wavelength sections $F(t, \lambda)$ were fit with a multiexponential decay model

$$F(t,\lambda) = \sum_i a_i(\lambda) \exp(-t/\tau_i)), \quad (2)$$

and the results of this fit were plotted as wavelength-dependent pre-exponential factors $a_i(\lambda)$ for each decay component with the corresponding characteristic decay time τ_i thus exhibiting the position of individual decay components in the spectrum. For a detailed description of the data evaluation and the calculation of the DAS, see [26].

All calculations were performed using the Origin 8.0 (OriginLab Corporation, United States) after fitting with Globals Unlimited (University of Illinois, Urbana, USA)® and SPCImage (Becker and Hickl, Germany) software packages.

Each experiment was repeated at least five times.

4. Results and discussion

Freezing of the CK_PBs was performed in the closed loop helium cryostat at a rate of 2–3 °C min^{-1}, which is a slow freezing (compared to freezing in liquid nitrogen) process [22]. As we have shown before [22], slow freezing may change the conformation of phycobiliproteins and chromophores bound to them, causing a strong reduction in its fluorescence lifetime (see Fig. 3A). The use of glycerol, which has cryoprotective properties, allows avoiding such consequences. It is important to note that some studies have shown that treatment with glycerol leads to uncoupling of energy transfer from PBs to chlorophyll due to the PB detachment from the thylakoid membrane [32]. However, in case of isolated PBs this effect is not of relevance. Fig. 3B shows the temperature dependence of the average fluorescence lifetimes of APC (663 nm) and TE (682 nm) in the CK_PBs. The temperature dependence of the average lifetime in the spectral channel corresponding to TE fluorescence (685 nm) is almost linear and doesn't demonstrate any nonlinear dependency or phase transition during freezing (Fig. 3B), indicating that no conformational changes occurred in the chromophore–protein structure and the sample retained its native conformation.

The characteristic average lifetime of the APC fluorescence is 1.6 ns at room temperature. When freezing isolated APC with cryoprotectant, its average fluorescence lifetime increases at low temperatures, however, as shown in Fig. 3B, in PBs (in the presence of TE) the APC fluorescence is quenched at low temperatures. Fluorescence quenching of APC in CK_PB cores is not related to the conformational changes of the APC pigment–protein complexes as observed in former studies for hydrated samples [22], see Fig. 3, as one can see that the character of temperature dependency of τ_{av} is very different from that of APC slow freezing (Fig. 3A). At the same time fluorescence decay curve for TE (at 685 nm) shows a pronounced fluorescence rise kinetics that is typical for donor–acceptor EET (Fig. 3C) [26]. At room temperature, preparations of PB cores and whole cells of the ΔPSI/ΔPSII mutant emit fluorescence with maximum intensity at 665 nm and show average lifetimes typical for APC. The decrease of temperature causes dramatic changes in fluorescence spectrum — the maximum shifts to 685 nm (see Fig. 4), suggesting that the APC fluorescence is strongly quenched due to the efficient EET to TE molecules.

The fluorescence spectra shown in Fig. 4 illustrate the differences between CK_PBs and the PBs in the ΔPSI/ΔPSII mutant. The ΔPSI/ΔPSII mutant has a broader fluorescence spectrum compared to the CK_PBs at room temperature. This fact is due to the lack of PC in the latter. Despite the fact that the number of PC is much higher than the number of APC [2], at room temperature the main fluorescence signal of ΔPSI/ΔPSII is emitted from APC, which is well explained by the temperature equilibration of the excited states between PC, APC and TE [3,26,33]. The energy gap between the excited states of PC and APC (0.06 eV) APC and TE (0.046 eV) is comparable to kT (0.026 eV at 300 K), allowing energy back transfer. At low temperatures, the probability of reverse energy transfer is reduced according to the small Boltzmann factor.

This phenomenon explains the fact that at 77 K the prevalent band in the fluorescence spectra corresponds to the TE emission. This conclusion is also confirmed by the analysis of the fluorescence decay kinetics and DAS (see Fig. 4B and D). At room temperature the blue part of fluorescence spectrum (~640 nm) of ΔPSI/ΔPSII mutant decays faster compared to CK_PBs (or to uncoupled phycobiliproteins for which characteristic average lifetime is 1.6 ns [34,35]) due to the presence of PC and effective EET from PC to APC.

Exposing the ΔPSI/ΔPSII sample to blue light at room temperature results in a slight increase of fluorescence intensity in the blue region of spectrum (Fig. 4C and E) that can be attributed to the spectral deformation caused by APC and TE quenching by activated OCP (see Fig. 4D and F), suggesting that PC fluorescence is not directly quenched by OCP [15] but only due to EET to APC.

At 77 K, no significant decrease in average fluorescence lifetime was observed upon the light adaptation of the ΔPSI/ΔPSII mutant.

A more detailed analysis of energy migration processes was made using the global analysis procedure [26]. Global analysis of CK_PB fluorescence (data not shown) reveals that the contribution of the fluorescence rise kinetics is most pronounced at low temperatures, indicating a highly efficient EET from APC to the TE. The increase of temperature leads to more diffusive (less directed) EET due to activation of the back energy transfer from APC to the TE.

Fig. 5 shows the DAS obtained by global analysis of the time resolved fluorescence spectra of the ΔPSI/ΔPSII mutant. At room temperature the DAS of dark adapted sample (DA RT) shows a distinctive fast (82 ps)

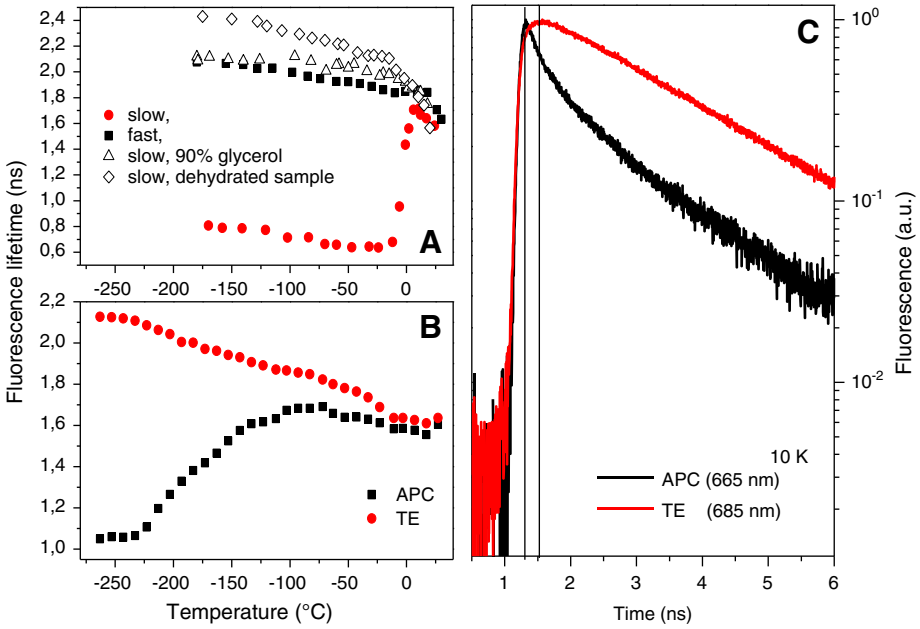

Fig. 3. (A) Temperature dependences of the average lifetime of APC during fast freezing (black squares), slow freezing (red circles), slow freezing in presence of glycerol (triangles) and during slow freezing of dehydrated sample (diamonds), detailed description in [22]. (B) Temperature dependence of the average lifetime of CK_PBs in spectral channels corresponding TE (685 nm) and APC (665 nm). (C) Fluorescence decay kinetics of TE (685 nm) and APC (665 nm) in the PB core at 10 K, vertical lines indicate ~200 ps shift of the maximum fluorescence intensity.

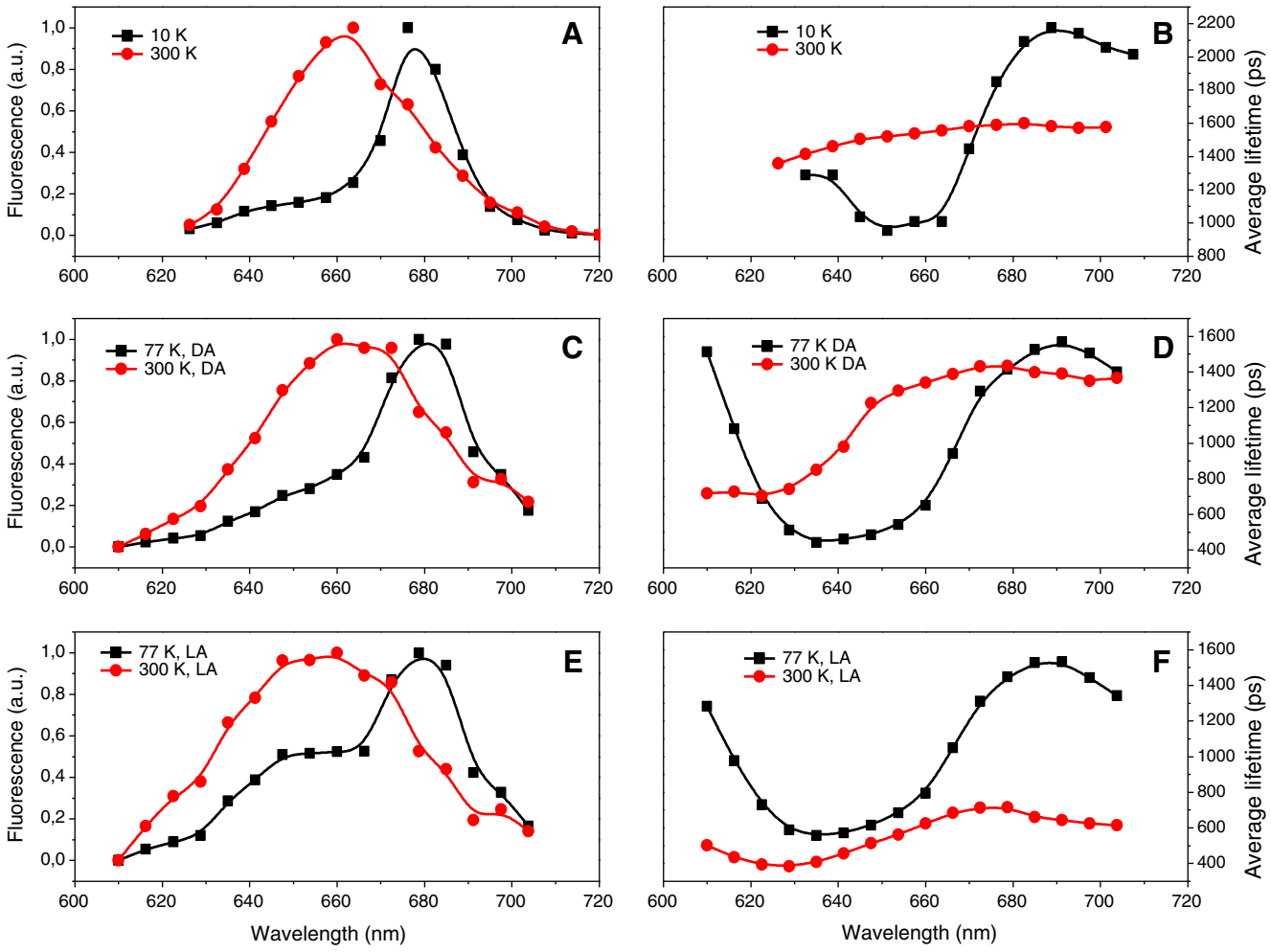

Fig. 4. Fluorescence spectra (on the left) and average lifetime in dependency of the emission wavelength (right side) of CK_PBs (A, B) and ΔPSI/ΔPSII mutant (C, D — dark adapted, E, F — light adapted sample, 5 min under photon flux densities of 1000 μmol photons m^{-2} s^{-1}) of *Synechocystis* sp. PCC6803 at 10 K (77 K for ΔPSI/ΔPSII) (black) and 300 K (red). The fluorescence intensity in the spectra is normalized to the maximum values. The excitation wavelength was 405 nm.

component with negative amplitude (Fig. 5A), characterizing the overall EET in the PC–APC–TE system. Here, we do not resolve the PC–APC EET process, which occurs on a 10 ps time scale [15,16], separately. The 0.97 and 1.98 ns components in the DAS of DA RT sample can be attributed to the temperature-equilibrated relaxation of the APC and TE pools. After adaptation to light the component with negative amplitude is not observed (Fig. 5B), while a new fast (170 ps) all-positive component appears in DAS, which can be attributed to the appearance of OCP-induced quenching in the system and subsequent dissipative depletion of the excited states by OCP. This fact is in agreement with the changes in DAS obtained in [15] for the wild type PB–OCP system. The 20 nm blue shift of the 170 ps component compared to the 1 ns component, indicative for the unquenched APC, in the LA RT DAS, indicates, according to the reduced quenching of the PC fluorescence (Fig. 4) and the data of Ref. [15], that the PC pool (with maximum in emission spectrum at 640 nm) is not the site of NPQ.

Since the time of the reverse transformation of OCP from its red to orange form is much longer than the time required to freeze the sample in liquid nitrogen, it is reasonable to assume that a large amount of OCP is in quenching state at 77 K. The 77 K DAS for the DA sample are analogous to the ones obtained at RT (159 ps component with negative amplitude centered at 680 nm responsible for EET in the PC–APC–TE system, 0.54 and 1.75 ns components responsible for the relaxation of APC and TE), though it can be seen that fast freezing of DA samples increases the efficiency of EET from APC to TE (Fig. 5C), which is very similar to effects observed on the PB core (see Fig. 3B). As the result, the maxima of the slow (0.54 and 1.75 ns) components are shifted towards the maximum of TE emission (680 nm).

In contrast to the RT experiments, the DAS of the 77 K LA sample with activated OCP is much more similar with the DAS for the 77 K DA sample (Fig. 5D): it also demonstrates the EET component (165 ps) with negative amplitude centered at 680 nm. A minor difference is the slightly bigger contribution of 0.6 ns component in the 650 nm region, probably indicating the decrease of APC average lifetime.

In literature, there is evidence that NPQ at 77 K is not as efficient as at room temperature. However, such estimates are obtained by changes in steady-state spectra, which require special reference signal or just normalization to specific wavelength [8,13,14,21,24]. In this case, the fluorescence lifetime analysis is more legitimate, because (unlike intensity) fluorescence lifetimes are associated with the quantum yield directly (which also allows one to compare the steady-state spectra at low temperatures).

The average lifetime of ΔPSI/ΔPSII mutant at 660 nm decreases from 1.4 to 0.6 ns for the DA RT and LA RT samples (Fig. 4), respectively, this corresponds to 60% NPQ. This observation is consistent with the changes of integral intensity shown in Fig. 6A. The change in the average lifetime for 77 K DA and LA samples (decrease from 0.8 to 0.64 ns) corresponds to 20% NPQ — this is also in consistency with the results of steady-state measurements (data not shown). This clearly show that OCP is not as efficient at 77 K as at room temperature that might be explained by conformational distortion of the OCP found at low temperature as it is observed for many photoactive pigment–protein complexes [36].

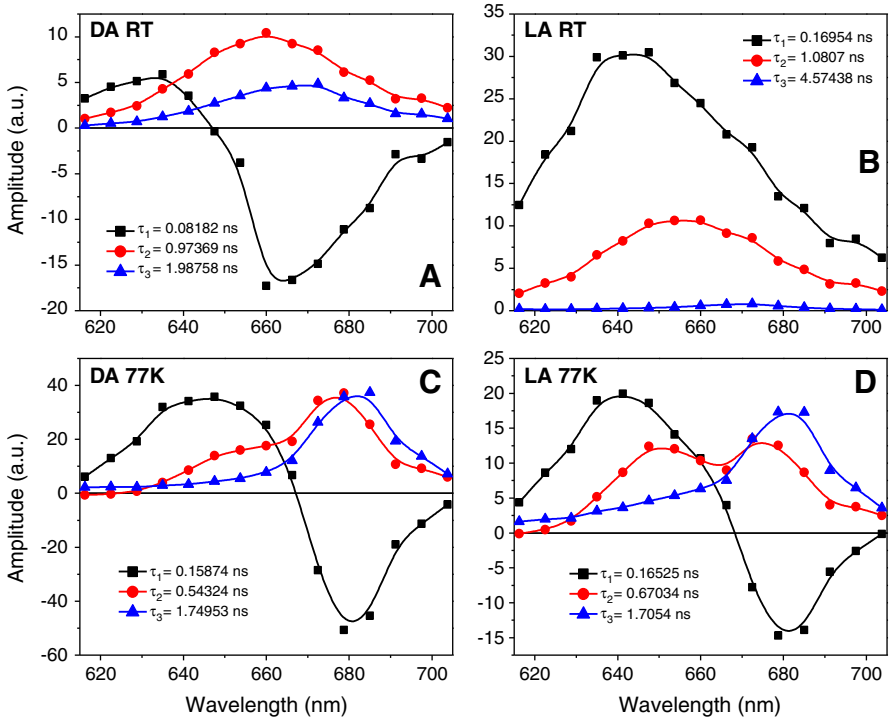

Fig. 5. Decay associated spectra of ΔPSI/ΔPSII mutant at 300 (RT) and 77 K dark adapted (DA) and after adaptation to blue light with the 3000 μmol photons m^{-2} s^{-1} (LA).

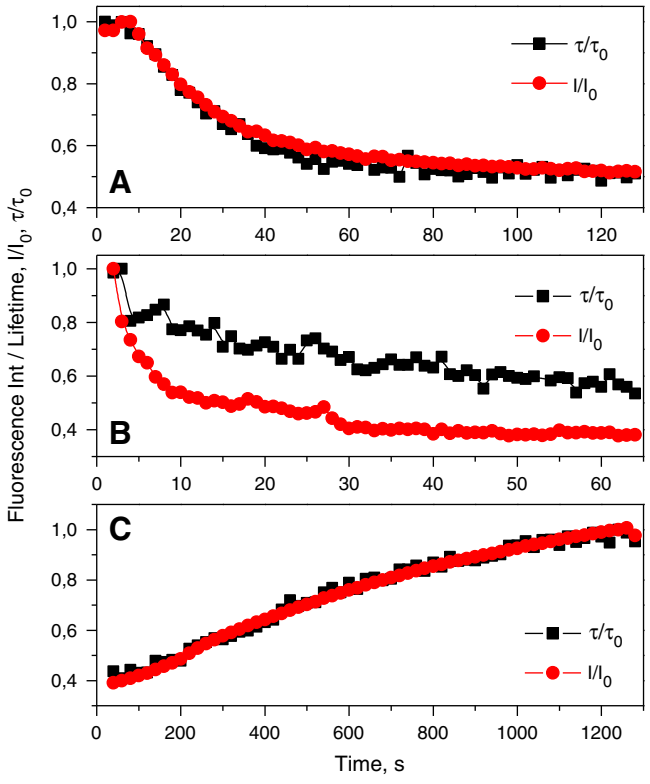

Fig. 6. The time course of fluorescence intensity (red) and fluorescence lifetime (black) of the ΔPSI/ΔPSII mutant during adaptation to blue light (A, 800 μmol photons m^{-2} s^{-1}, 475 nm LED, and B, 2000 μmol photons m^{-2} s^{-1}, 405 nm pulsed laser (60 ps, 20 MHz)) and during the transition into the dark adapted state (C). Fluorescence decay curves were measured using 405 nm laser pulses (50 MHz, 26 ps, 13 pJ). For A and B, the initial values of the intensities and lifetimes were set as unity. For C final intensities and lifetimes were set as unity.

The availability of ΔPSI/ΔPSII mutant allowed us not only to compare the fluorescence lifetimes at different temperatures, but also to study the transition dynamics from a dark adapted to light adapted state *in vivo*. We investigated how the intensity of blue light, which activates the OCP, affects the fluorescence dynamics of PC, APC and TE pools. This allowed us to draw conclusions on the dynamics of NPQ and fluorescence recovery at room temperature.

The typical time course of fluorescence quenching under actinic light irradiation is presented in Fig. 6A–B (red curves). At low light intensities (Fig. 5A, 800 μmol photons m^{-2} s^{-1}) the quenching curve can be fitted with monoexponential decay, while for the photon flux density values higher than physiological ones (Fig. 5B, 2000 μmol photons m^{-2} s^{-1}) multiexponential fitting is required. The amplitude of NPQ is determined by the number of OCP molecules per single PB [7,37] and was about 50% in this work.

Simultaneously with fluorescence intensity, the fluorescence decay curves were measured at different irradiation times. A set of typical fluorescence decay curves obtained during LA to DA transition (fluorescence recovery in darkness) is presented in Fig. 7. Here, the registration wavelength was chosen to be 660 nm because as it was shown in [6] the site of OCP-induced fluorescence quenching is likely to be on APC. Fluorescence decay curves obtained during irradiation with blue light (DA to LA transition) demonstrated the similar trend, however, in this case acquisition time (2 s) and signal-to-noise ratio were smaller as the NPQ induced process occurs faster compared to fluorescence recovery in darkness.

The fluorescence decay curve in Fig. 7, obtained for the LA sample (the lowest curve in Fig. 7), demonstrates the strong excited state depopulation, and the appearance of a fast decay component(~150 ps) which can attributed to the APC–OCP EET. This component can be also seen in the DAS for the LA RT sample (Fig. 5B). In fluorescence decay curves shown in Fig. 7 a very long component was also observed with an average lifetime of 4 ns and small amplitude less than 2%. This fact can be explained by the presence of the residual chlorophyll in the ΔPSI/ΔPSII mutant [24].

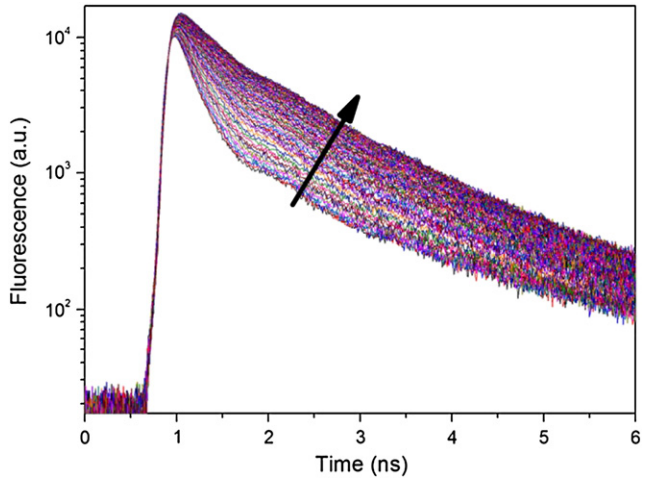

Fig. 7. Fluorescence decay curves obtained for the LA to DA transition of ΔPSI/ΔPSII mutant (fluorescence recovery after 5 min irradiation with 1000 μmol photons m^{-2} s^{-1} 475 nm blue light). Registration wavelength = 660 ± 3.12 nm, integration time was set to 20 s for each of 64 cycles. The arrow indicates fluorescence recovery.

The dependence of the average lifetime of the sample on the duration of irradiation is presented in Fig. 6A–C with black dots. The dynamics of changes in the fluorescence intensity and average lifetime match almost perfectly (Fig. 6A). Only in the case of high intensity light illumination it can be observed that the change in the average fluorescence lifetime (OCP activation) is accompanied by a secondary effect that leads to an additional reduction of the fluorescence intensity but not to an additional reduction of the fluorescence lifetime. Thus, the difference between the curves in Fig. 6B is caused by photobleaching under high light intensities far exceeding physiological values and is not related to NPQ. The subsequent recovery of fluorescence during the sample's adaptation to darkness also demonstrates the match of the dependencies of fluorescence intensity and average lifetime on time (Fig. 6C). It is important to note that the rate of fluorescence recovery in the darkness is at least an order of magnitude slower than the rate of NPQ caused by OCP photoactivation (Fig. 6A–C) — this result is in agreement with literature data [7].

As in the majority of works, devoted to the OCP-induced NPQ [7,11,14,15,24,38], our results elucidate the role of APC to OCP excitation transfer in quenching of PB fluorescence. At the same time, in [15,16] authors imply the ultrafast (<1 ps) character of this process, performing multistep processing of experimental data. This procedure included target analysis and the division of the obtained EET rate by the number of APC subunits in the PBs (66) to take into account excitation migration in the APC pool. However, here we didn't focus on the mechanism of energy transfer from APC to OCP and used the EET rates obtained directly from the fluorescence decay curves at different irradiations/recoveries in darkness times to study the time course of NPQ.

We observed the gradual increase of the rate of the fast component in APC fluorescence decay upon irradiation of the sample with blue light, followed by the gradual decrease of this component's rate during the adaptation of the sample to darkness. Moreover, the time course of the decrease in the fluorescence intensity during irradiation of the sample with blue light matches closely to the changes in the average fluorescence lifetime during NPQ induction (Fig. 6A) and consequent fluorescence recovery (Fig. 6C).

Assuming that a) the rate of APC–OCP EET is independent on the rate of excitation migration in the APC pool and b) EET from each APC molecule to the OCP occurs in one step we consider two possible mechanisms of EET:

1. Investigated system is described by two components including non-quenched and quenched species of PBs with fixed fluorescence lifetimes of τ and $(1/\tau + K)^{-1}$, respectively, where K is the rate of APC–OCP EET.
2. The rate of APC–OCP EET is time-dependent and is determined by the process of OCP incorporation into PBs which is regulated by conformational changes of proteins. In this case, an increase of the EET rate should be observed during the activation of NPQ as the EET becomes more efficient in time, followed by a decrease of the EET rate constant during fluorescence recovery (when OCP detaches from PBs).

To compare between these two models we performed fits of the fluorescence decay curves measured at different irradiation times both with fixed fluorescence lifetimes, taken from DAS, and with the three components with unfixed lifetimes. If model 1 holds one would expect that these lifetimes are suitable to fit all decay curves and only the amplitude of the fast fluorescence component is rising in time.

The results of our fit of the fluorescence decay curves suggests that the second model, involving the change of energy transfer rate in time, is more reliable, and the corresponding χ^2 values are approximately 15% smaller than in the case of the first (two-component) model. We consider that this observation indicates the role of intermolecular interactions between the red form of OCP and PB's binding site as the signature of conformational changes that result in the gradual change of the EET rate in time.

5. Conclusion

In this paper we have investigated the time course of NPQ in *Synechocystis* sp. PCC6803 using picosecond time-resolved fluorimetry. The dependencies of fluorescence intensity and average fluorescence lifetime of APC on blue light irradiation/recovery in darkness were found to match almost perfectly, indicating an efficient APC → OCP EET. It was shown that upon activation of OCP a fast component in the fluorescence decay appears, and its rate gradually changes upon the sample illumination or fluorescence recovery in darkness. The maximum rate of this component was estimated to be $(170\ ps)^{-1}$ from the data shown in Fig. 5. In addition it was observed that this rate constant changes during the adaption process to the light and/or dark adapted state.

We interpret the time dependence of the EET rate as the consequence of the process of interaction between OCP and PBs that occurs concomitant to conformational changes of the protein.

It was shown by the time-resolved measurements that the rate of EET from APC to OCP is significantly reduced at low temperatures, that is in agreement with steady-state fluorimetry data. We consider that this fact also indicates the role of the proteins conformation for effective interaction between OCP–PBs and efficient NPQ. Efficient NPQ occurs only at room temperature.

Acknowledgements

The authors express their sincere gratitude to Doctor G. Ajlani for kindly providing mutants CK and Professor W.F.J. Vermaas for ΔPSI/ΔPSII mutant. The financial support by BMBF RUS 10/026 is gratefully acknowledged. V.Z. Paschenko, E.G. Maksimov and I.V. Elanskaya thank the Russian Foundation for Basic Research (project 11-04-01617, 12-04-31100 and 12-04-00603-a), OPTEC and Center of National Intellectual Reserve for partial support of this work. F-J. Schmitt and T. Friedrich acknowledge the financial support by BMBF project "Quantum" (FKZ 13N10076) and COST for financial support in the framework of COST action MP1205. E.A. Shirshin thanks the Russian Foundation for Basic Research (project 12-05-31388). The authors are also grateful to Dr. F.I. Kouzminov for valuable comments on the manuscript.

References

[1] D.A. Bryant, G. Guglielmi, N.T. Marsac, A.-M. Castets, G. Cohen-Bazire, The structure of cyanobacterial phycobilisomes: a model, Arch. Microbiol. 123 (1979) 113–127.
[2] R. MacColl, Cyanobacterial phycobilisomes, J. Struct. Biol. 124 (1998) 311–334.

[3] C.W. Mullineaux, A.R. Holzwarth, Kinetics of excitation energy transfer in the cyanobacterial phycobilisome-photosystem II complex, Biochim. Biophys. Acta 1098 (1991) 68–78.
[4] K.K. Niyogi, Photoprotection revisited: genetic and molecular approaches, Annu. Rev. Plant Physiol. Plant Mol. Biol. 50 (1999) 333–359.
[5] E.G. Maksimov, F.I. Kuzminov, I.V. Konyuhov, I.V. Elanskaya, V.Z. Paschenko, Photosystem 2 effective fluorescence cross-section of cyanobacterium *Synechocystis* sp. pcc6803 and its mutants, J. Photochem. Photobiol. B Biol. 104 (2011) 285–291.
[6] J. Biggins, D. Bruce, Regulation of excitation energy transfer in organisms containing phycobilins, Photosynth. Res. 20 (1989) 1–34.
[7] D. Kirilovsky, C.A. Kerfeld, The orange carotenoid protein: a blue-green light photoactive protein, Photochem. Photobiol. Sci. 12 (2013) 1135–1143.
[8] A. Wilson, G. Ajlani, J.-M. Verbavatz, I. Vass, C.A. Kerfeld, D. Kirilovsky, A soluble carotenoid protein involved in phycobilisome-related energy dissipation in cyanobacteria, Plant Cell 18 (2006) 992–1007.
[9] T.K. Holt, D.W. Krogmann, A carotenoid protein from cyanobacteria, Biochim. Biophys. Acta 637 (1981) 408–414.
[10] C.A. Kerfeld, M.R. Sawaya, V. Brahmandam, D. Cascio, K.K. Ho, C.C. Trevitchik-Sutton, D.W. Krogman, T.O. Yeates, The crystal structure of a cyanobacterial water-soluble carotenoid binding protein, Structure 11 (2003) 55–65.
[11] M.Y. Gorbunov, F.I. Kuzminov, V.V. Fadeev, J.D. Kim, P.G. Falkowski, A kinetic model of non-photochemical quenching in cyanobacteria, Biochim. Biophys. Acta 1807 (2011) 1591–1599.
[12] F.I. Kuzminov, N.V. Karapetyan, M.G. Rakhimberdieva, I.V. Elanskaya, M.Y. Gorbunov, V.V. Fadeev, Investigation of OCP-triggered dissipation of excitation energy in PSI/PSII-less *Synechocystis* sp. PCC 6803 mutant using non-linear laser fluorimetry, Biochim. Biophys. Acta 1817 (2012) 1012–1021.
[13] M. Gwizdala, A. Wilson, D. Kirilovsky, In vitro reconstitution of the cyanobacterial photoprotective mechanism mediated by the orange carotenoid protein in *Synechocystis* PCC 6803, Plant Cell 23 (2011) 2631–2643.
[14] M.G. Rakhimberdieva, I.V. Elanskaya, W.F.J. Vermaas, N.V. Karapetyan, Carotenoid-triggered energy dissipation in phycobilisomes of *Synechocystis* sp. PCC 6803 diverts excitation away from reaction centers of both photosystems, Biochim. Biophys. Acta 1797 (2010) 241–249.
[15] L. Tian, M. Gwizdala, I.H.M. van Stokkum, R.B.M. Koehorst, D. Kirilovsky, H. van Amerongen, Picosecond kinetics of light harvesting and photoprotective quenching in wild-type and mutant phycobilisomes isolated from the cyanobacterium *Synechocystis* PCC 6803, Biophys. J. 102 (2012) 1692–1700.
[16] L. Tian, I.H.M. van Stokkum, R.B.M. Koehorst, A. Jongerius, D. Kirilovsky, H. van Amerongen, Site, rate, and mechanism of photoprotective quenching in cyanobacteria, J. Am. Chem. Soc. 133 (2011) 18304–18311.
[17] M. Gwizdala, A. Wilson, A. Omairi-Nasser, D. Kirilovsky, Characterization of the *Synechocystis* PCC 6803 fluorescence recovery protein involved in photoprotection, Biochim. Biophys. Acta (2013) 348–354.
[18] M.G. Rakhimberdieva, Y.V. Bolychevtseva, I.V. Elanskaya, N.V. Karapetyan, Protein–protein interactions in carotenoid triggered quenching of phycobilisome fluorescence in *Synechocystis* sp. PCC 6803, FEBS Lett. 581 (2007) 2429–2433.
[19] C.A. Kerfeld, D. Kirilovsky, Photoprotection in cyanobacteria: The orange carotenoid protein and energy dissipation, in: G.A. Peschek, C. Obinger, G. Renger (Eds.), Bioenergetic Processes of Cyanobacteria, Springer, Dodrecht, 2011.
[20] I.N. Stadnichuk, M.F. Yanyushin, E.G. Maksimov, E.P. Lukashev, S.K. Zharmukhamedov, I.V. Elanskaya, V.Z. Paschenko, Site of non-photochemical quenching of the phycobilisome by orange carotenoid protein in the cyanobacterium *Synechocystis* sp. PCC 6803, Biochim. Biophys. Acta 1817 (2012) 1436–1445.
[21] D. Jallet, M. Gwizdala, D. Kirilovsky, ApcD, ApcF and ApcE are not required for the orange carotenoid protein related phycobilisome fluorescence quenching in the cyanobacterium *Synechocystis* PCC 6803, Biochim. Biophys. Acta 1817 (2011) 1418–1427.
[22] E.G. Maksimov, F.-J. Schmitt, P. Hatti, K.E. Klementiev, V.Z. Paschenko, G. Renger, A.B. Rubin, Anomalous temperature dependence of the fluorescence lifetime of phycobiliproteins, Laser Phys. Lett. 10 (2013) 055602.
[23] G. Ajlani, C. Vernotte, Construction and characterization of phycobiliprotein-less mutant of *Synechocystis* sp. PCC 6803, Plant Mol. Biol. 37 (1998) 577–580.
[24] M.G. Rakhimberdieva, F.I. Kuzminov, I.V. Elanskaya, N.V. Karapetyan, *Synechocystis* sp. PCC 6803 mutant lacking both photosystems exhibits strong carotenoid-induced quenching of phycobilisome fluorescence, FEBS Lett. 585 (2011) 585–589.
[25] A. Wilson, C. Punginelli, M. Couturier, F. Perreau, D. Kirilovsky, Essential role of two tyrosines and two tryptophans on the photoprotection activity of the Orange Carotenoid Protein, Biochim. Biophys. Acta 1807 (2011) 293–301.
[26] F.-J. Schmitt, Picobiophotonics for the Investigation of Pigment–Pigment and Pigment–Protein Interactions in Photosynthetic Complexes, (thesis) Technische Universität Berlin, 2011. (http://opus.kobv.de/tuberlin/volltexte/2011/3202/pdf/schmitt_franzjosef.pdf).
[27] R. Rippka, J. Deruelles, J.B. Waterbury, M. Herdman, R.Y. Stanier, Generic assignments, strain histories and properties of pure cultures of cyanobacteria, J. Gen. Microbiol. 111 (1979) 1–61.
[28] S. Ermakova-Gedes, S. Shestakov, W. Vermaas, in: P. Mathis (Ed.), Photosynthesis: From Light to Biosphere, 1, Kluwer Academic Publishers, Dordrecht, The Netherlands, 1995, pp. 483–486.
[29] J.C. Thomas, B. Ughy, B. Lagoutte, G. Ajlani, A second isoform of the ferredoxin: NADP oxidoreductase generated by an in-frame initiation of translation, Proc. Natl. Acad. Sci. U. S. A. 103 (2006) 18368–18373.
[30] Becker & Hickl GmbH, PML-16-C 16 Channel Detector Head for Time-correlated Single Photon Counting, User Handbook, Berlin, 2006. (http://www.becker-hickl.de/pdf/pml16c21.pdf).
[31] E.G. Maksimov, G.V. Tsoraev, V.Z. Paschenko, A.B. Rubin, The nature of anomalous temperature dependence of the fluorescence lifetime of allophycocyanin, Dokl. Biochem. Biophys. 443 (2012) 86–90.
[32] Hai-Bin Mao, Guo-Fu Li, Dong-Hai Li, Qing-Yu Wu, Yan-Dao Gong, Xiu-Fang Zhang, Nan-Ming Zhao, Effects of glycerol and high temperatures on structure and function of phycobilisomes in *Synechocystis* sp. PCC 6803, FEBS Lett. 553 (2003) 68–72.
[33] C. Theiss, F.-J. Schmitt, J. Pieper, C. Nganou, M. Grehn, M. Vitali, R. Olliges, H.J. Eichler, H.-J. Eckert, Excitation energy transfer in intact cells and in the phycobiliprotein antennae of the chlorophyll d containing cyanobacterium *Acaryochloris marina*, J. Plant Physiol. 168 (2011) 1473–1487.
[34] J.R. Lakowicz, Principles of Fluorescence Spectroscopy, 2nd ed. Kluwer Academic/Plenum Publishers, 1999. 465.
[35] R.H. Goldsmith, W.E. Moerner, Watching conformational- and photodynamics of single fluorescent proteins in solution, Nat. Chem. 2 (2010) 179–186.
[36] J. Pieper, T. Hauss, A. Buchsteiner, K. Baczynski, K. Adamiak, R.E. Lechner, G. Renger, Temperature- and hydration-dependent protein dynamics in photosystem II of green plants studied by quasielastic neutron scattering, Biochemistry 46 (2007) 11398–11409.
[37] A. Wilson, C. Punginelli, A. Gall, C. Bonetti, M. Alexandre, J.-M. Routaboul, C.A. Kerfeld, R. van Grondelle, B. Robert, J.T.M. Kennis, D. Kirilovsky, A photoactive carotenoid protein acting as light intensity sensor, PNAS 105 (2008) 12075–12080.
[38] R. Berera, I.H. van Stokkum, M. Gwizdala, A. Wilson, D. Kirilovsky, R. van Grondelle, The photophysics of the orange carotenoid protein, a light-powered molecular switch, J. Phys. Chem. B 116 (2012) 2568–2574.
[39] F.J. Schmitt, E.G. Maksimov, C. Junghans, J. Weisenborn, P. Hatti, V.Z. Paschenko, S.I. Allakhverdiev, T. Friedrich, Structural organization and dynamic processes in protein complexes determined by multiparameter imaging, Signpost Open Access J. Nano Photo Biosci. 1 (2013) 1–47.